

# Conversion efficiency calculations for EUV radiation emitted from laser-produced Tin plasmas

Betül ATALAY<sup>1</sup>, Necla KENAR<sup>2</sup>, Arif DEMİR<sup>3</sup>

<sup>1</sup>*Çanakkale Onsekiz Mart University, Çanakkale-TURKEY*

*e-mail: batalay@comu.edu.tr*

<sup>2</sup>*University of Kocaeli, Kocaeli-TURKEY*

<sup>3</sup>*Laser Technologies Research and Application Center, Kocaeli-TURKEY*

Received 06.03.2008

## Abstract

Ni-like and Co-like EUV radiation between 11–17 nm emitted from laser produced tin plasmas was modelled by using the hydrodynamic/atomic physics code EHYBRID. The atomic data were obtained using the Cowan code. The effects of driving laser pulse duration and the laser intensity with different wavelengths were investigated. The maximum conversion efficiency was calculated as 13.4% for a 266 nm Nd:YAG laser with  $1 \times 10^{13}$  W/cm<sup>2</sup> pulse intensity and 5 ns pulse duration.

**Key Words:** Laser produced plasmas, plasma simulation, extreme ultraviolet radiation, lithography.

**PACS:** 52.50.Jm, 52.65.-y, 52.25.Os, 85.40.Hp.

## 1. Introduction

The interaction of short, intense laser pulses with solid targets has been extensively studied in recent decades. Laser-produced plasmas are now well proven as suitable lasing media for X-ray lasers [1, 2]. High-intensity laser produced plasmas attract particular attention as extreme ultraviolet emission sources for lithography of next generation semiconductors [3]. Next generation semiconductors based on extreme ultraviolet lithography (EUVL) will require bright, efficient radiation sources at wavelengths near 13.5 nm [4]. This requirement is driven by the use of Mo/Si multilayer mirrors in the optical system of EUVL [5]. One of the crucial factors in developing radiation sources for EUVL is the conversion efficiency (CE) from laser light into the EUV radiation. A suitable radiation source must achieve at least 3% conversion efficiency for making EUVL economically affordable [6].

Among the various target materials tin is considered to be the most efficient radiator due to its compactness and high emissivity [7]. Emission of laser produced tin plasmas arises from 4d–4f, 4p–4d and 4d–5p

transitions of tin ions with ionization charge state 8+ to 13+. In particular,  $4p^6 4d^N - 4p^5 4d^{N+1} + 4p^6 4d^{N-1}$  4f transition arrays of  $\text{Sn}^{5+}$  to  $\text{Sn}^{13+}$  ( $9 \geq N \geq 1$ ) produce intense quasi-continua (unresolved transition arrays (UTAs) [8] near 13.5 nm [9]. It was demonstrated that these sources match technology requirements [10]. The atomic data, however, is quite few for higher charge states; for more than 13+ there is increasing need for a database of EUV radiation from highly charged tin ions [11, 12].

In this work, we investigated EUV radiation from Ni-like and Co-like tin ions. The main interest is to increase the conversion efficiency for the optimization of the plasma conditions. To achieve that, conversion efficiencies with respect to variation of the variety of laser intensity, wavelength and pulse duration were calculated.

## 2. Modelling

The laser interaction with solid target and expansion of the subsequent plasma is simulated by the EHYBRID 1.5 dimensional hydrodynamic/atomic physics modelling software [13]. EHYBRID is a Lagrangian code that uses 98 spatial cells in the direction away from the target surface. Hence, the plasma can be modelled in the direction parallel to the driving laser in these spacial cells. The plasma, in each cell is assumed to be isothermal and the transverse expansion of the plasma is considered to be self-similar. In the self-similar approach, thermal conduction maintains a uniform temperature over transverse planes, and the velocity and density profiles along the transverse axes assume linear and Gaussian forms, respectively [13]. EHYBRID evaluates the absorption of laser energy through inverse bremsstrahlung and resonance absorption. Absorption of laser energy through inverse bremsstrahlung is calculated for each cell of plasma until it reaches the critical surface. Resonance absorption is calculated by assuming a 30% dump of the laser energy reaching the critical surface. The remainder of the energy is reflected back and inverse bremsstrahlung absorption is calculated for the reflected beam as it propagates back out of the plasma [14].

The code calculates, at each time step and for each cell, electron temperatures, electron densities and ionic fractions from neutral to bare nuclei using a detailed set of collisional-radiative equations and atomic level populations. To calculate the Ni-like and Co-like populations, all the collisional and the radiative processes such as collisional and radiative excitation/de-excitation, collisional ionization, radiative recombination, three-body and di-electronic recombination are taken into account. 222 Ni-like  $1s^2 2s^2 2p^6 3s^2 3p^6 3d^{10} - 1s^2 2s^2 2p^6 3s^2 3p^6 3d^9$  nl and 507 Co-like  $1s^2 2s^2 2p^6 3s^2 3p^6 3d^9 - 1s^2 2s^2 2p^6 3s^2 3p^6 3d^8$  nl resonance line intensities were calculated for the simulation of the spectral emission from the tin plasma.

The opacity is estimated by using an escape factor based on the Holstein function for Doppler broadened lines [15, 16]. Line intensities of spectral lines at a particular time are evaluated using

$$I_{\text{tot}} = \sum_{i,j} N_i \frac{hc}{\lambda_o} T A_{ij} \Delta V, \quad (1)$$

where  $N_i$  is the upper state population for a given transition,  $A_{ij}$  is the radiative transition probability for the transition,  $h$  is Planck's constant,  $c$  is the vacuum speed of light,  $T$  is an escape factor,  $\lambda_o$  is the spectral line wavelength and  $\Delta V$  is the volume of each cell and the summation is over the EHYBRID cells. Atomic data for Ni- and Co-like ions are calculated using the code developed by Cowan [17].

A series of simulations for laser produced tin plasmas were done to show how the laser parameters affect the conversion efficiency.

### 3. Results

In this study, 1.2 ns Nd:YAG laser pulses at fundamental wavelength, 2<sup>nd</sup>, 3<sup>rd</sup> and 4<sup>th</sup> harmonics were used to generate plasmas. A 100  $\mu\text{m}$  wide, 20  $\mu\text{m}$  thick and 1 cm long tin ribbon was used as a target. The laser intensity was changed between  $5 \times 10^{12}$  W/cm<sup>2</sup> and  $1 \times 10^{14}$  W/cm<sup>2</sup>. The emissivity of the plasma originated from bound-bound, bound-free and free-free transitions. The major contribution comes from the bound-bound transitions. Figure 1 shows the simulated time and space integrated Ni-like and Co-like spectrum between 110–172 Å. We got spectral lines at 138 Å and 139 Å originating from Ni-like tin ions, which could be used in the development of EUVL.

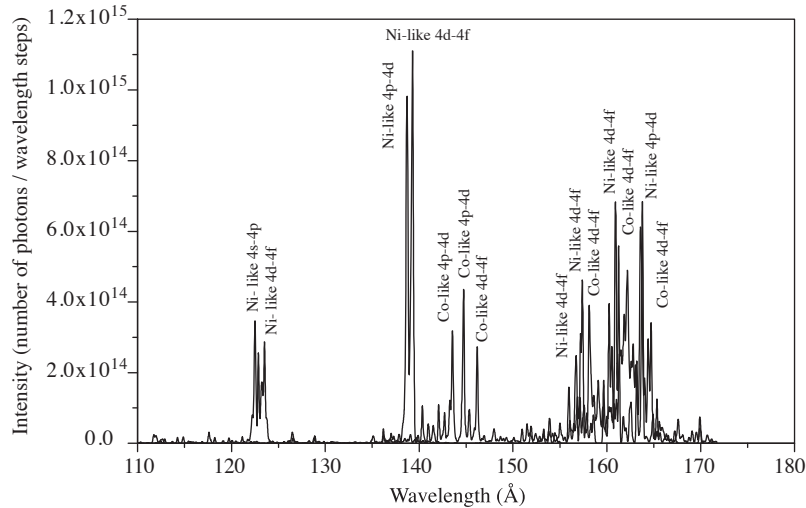


**Figure1.** The simulated Ni-like and Co-like spectrum emitted from laser produced tin plasmas.

In addition to spectral line intensities, free-free and free-bound transitions were taken into account for the emissivity of the plasma. Free-free and free-bound transitions resulting from recombination of free electrons with Zn, Cu-, Ni-, Co- and Fe-like ions were calculated from EHYBRID deduced plasma parameters in our post-processor. The time integrated continuum spectrum obtained from free-free and free-bound is shown in Figure 2.

The parameters: laser pulse energy, laser wavelength and the laser pulse duration were varied. The effect of laser intensity on the conversion efficiency of EUV emission from laser produced tin plasmas was investigated by changing laser intensity from  $5 \times 10^{12}$  W/cm<sup>2</sup> to  $1 \times 10^{14}$  W/cm<sup>2</sup>. The range of laser intensity was chosen to optimize the Ni-like and Co-like ionization of tin. At low intensities, Ni- and Co-like ionization stages did not appear. The laser pulse duration was fixed to 1.2 ns. The change of conversion efficiency as a function of laser intensity is shown in Figure 3.

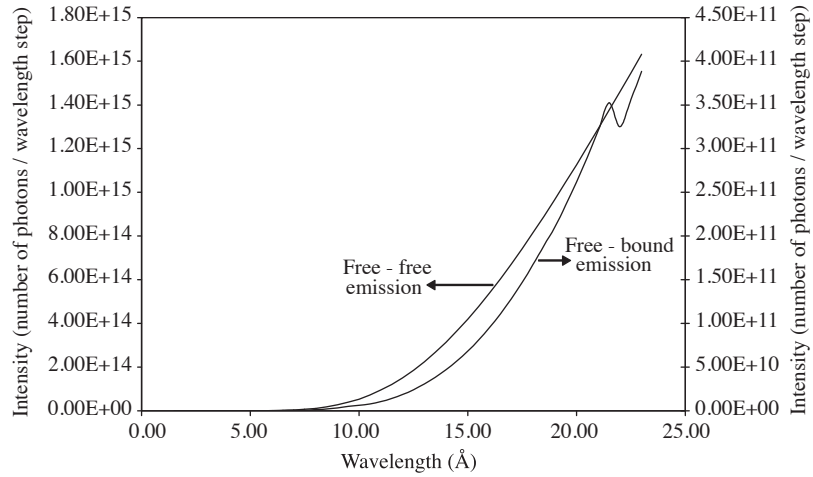


**Figure 2.** The time-integrated free-free and free-bound emission from the Zn, Cu-, Ni-, Co- and Fe-like ions.

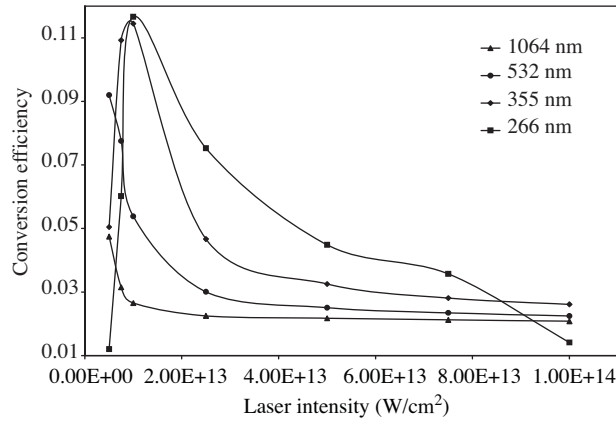


**Figure 3.** The conversion efficiency with respect to laser intensity.

The maximum conversion efficiency of laser energy into EUV was calculated to be 4.74% for  $5 \times 10^{12}$  W/cm<sup>2</sup> pulse intensity at the fundamental wavelength and 9.2% for  $5 \times 10^{12}$  W/cm<sup>2</sup> pulse intensity at the 2<sup>nd</sup> harmonic. At the 3<sup>rd</sup> and the 4<sup>th</sup> harmonic of the laser with  $1 \times 10^{13}$  W/cm<sup>2</sup> pulse intensity, the maximum conversion efficiencies were calculated as 11.4% and 11.7%, respectively. The conversion efficiencies were calculated for the 11–17 nm regions. It is understood from the figure that the conversion efficiency of laser light to Ni- like and Co-like EUV radiation decreases with increasing laser intensity. At higher intensities, there are not only Ni- and Co-like tin ions but also tin ions with different charge states present, which causes lower conversion efficiency values. Figure 3 also shows that the 3<sup>rd</sup> and the 4<sup>th</sup> harmonics of the Nd:YAG laser have better conversion efficiencies than the 2<sup>nd</sup> harmonic and the fundamental wavelength of the laser. This situation comes from the fact that the critical density is proportional to  $1/\lambda^2$  in laser produced plasmas. As a result, short wavelengths can penetrate into higher density; therefore, they get better conversion efficiency than longer wavelengths.

For maximizing conversion efficiency of EUV emission, laser pulse duration was varied between 5–30 ns, with 1064 nm laser for  $1 \times 10^{13}$  W/cm<sup>2</sup> pulse intensity. Figure 4 shows the variation of conversion efficiency

with the laser pulse duration. Conversion efficiency increases with the pulse duration and maximum conversion efficiency is found to be 8.75% at 20 ns. However, after 20 ns conversion efficiency began to decrease.

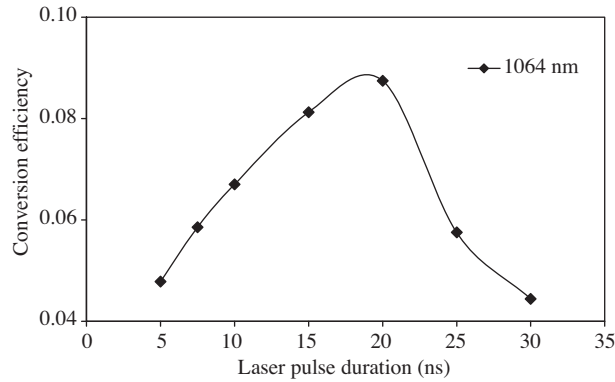


**Figure 4.** The conversion efficiency as a function of laser pulse duration.

The change of conversion efficiency with respect to laser pulse durations at 266 nm wavelength is shown at Figure 5. As shown in the figure conversion efficiency takes a maximum value of 13.4% at 5 ns and decreases with increasing pulse duration.

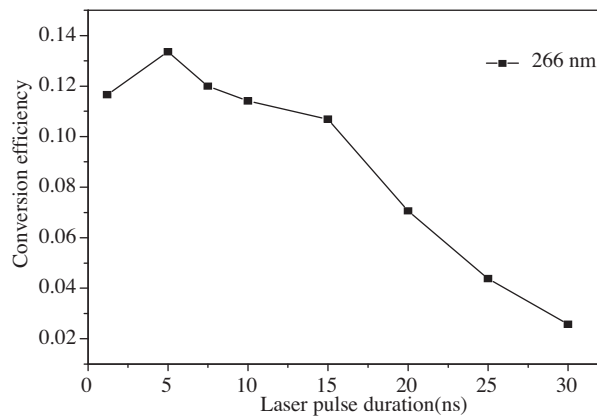


**Figure 5.** The conversion efficiency as a function of laser pulse duration at 266 nm.

## 4. Conclusion

In this study, a series of radiation-hydrodynamics simulations was performed for laser produced tin plasmas to examine the dependence of the conversion efficiency on the laser intensity, wavelength and pulse duration. The maximum conversion efficiency was calculated as 13.4% for the 266 nm Nd:YAG laser with  $1 \times 10^{13}$  W/cm<sup>2</sup> pulse intensity and 5 ns pulse duration. The results revealed that with increasing wavelength, the maximum conversion efficiency can be increased by decreasing the laser intensity. For the experimental studies, Q-switched Nd:YAG lasers at a wavelength of 1064 nm with typical laser pulse energies in the range of 0.5–1.0 J, and pulse durations of 10 ns, at 10 Hz operation and the focussed beam size  $\sim 100$   $\mu$ m can be used as convenient and effective laser drivers.

## References

- [1] G.J. Tallents, *J. Phys. D: Appl. Phys.*, **36**, (2003) R259.
- [2] R.C. Elton, *X-Ray Lasers*, (Academic press, San Diego, 1990).
- [3] V. Bakshi, *EUV Sources for Lithography*, (SPIE Press, Washington, 2005).
- [4] Y. Watanabe, K. Ota, and H. Franken., *Proceedings of the EUV Source Workshop, International Sematech*, Santa Clara, (2004).
- [5] J. J. MacFarlane, C. L. Rettig, P. Wang, I. E. Golovkin, and P. R. Woodruff, *Proc. SPIE*, **5751**, (2005), 588.
- [6] S. S. Harilal, B. O'Shay, M. S. Tillack, Y. Tao, R. Paguio, A. Nikroo and C. A. Back, *J. Phys. D: Appl. Phys.*, **39**, (2006), 484.
- [7] K. Nishihara et al., *Proc. of the 3rd Int. Sematech EUVL Symp*, Miyazaki, (2004).
- [8] P. Mandlebaum, M. Finkenthal, J. L. Schwob and M. Klapisch, *Phys. Rev. A*, **35**, (1987), 5051.
- [9] G. O'Sullivan and R. Faulkner, *Opt. Eng.*, **33**, (1994), 3978.
- [10] K. Nishihara et al., *Phys. Plasmas*, **15**, (2008), 056708.
- [11] C. Suzuki et al., *Journal of Physics: Conference Series*, **163**, (2009), 012019.
- [12] A. Sasaki et al., *High Energy Density Physics*, **3**, (2007) 250.
- [13] G.J. Pert, *J. Fluid Mech*, **131**, (1983), 401.
- [14] P.B. Holden et al, *J. Phys. B: At. Mol. Opt. Phys.*, **27**, (1994), 341.
- [15] T. Holstein, *Phys. Rev.*, **72**, (1947), 1212.
- [16] T. Holstein, *Phys. Rev.*, **83**, (1951), 1159.
- [17] R. D. Cowan, *J. Opt. Soc. Am.*, **58**, (1968), 808.